PAPER

Vortex fluidic mediated synthesis of polysulfone†‡

Aghil Igder, [ab] Scott Pye, [b] Ahmed Hussein Mohammed Al-Antaki, [b] Alireza Keshavarz, [a] Colin L. Raston *[b] and Ata Nosrati[a]

Polysulfone (PSF) was prepared under high shear in a vortex fluidic device (VFD) operating in confined mode, and its properties compared with that prepared using batch processing. This involved reacting the pre-prepared disodium salt of bisphenol A (BPA) with a 4,4′-dihalodiphenylsulfone under anhydrous conditions. Scanning electron microscopy (SEM) established that in the thin film microfluidic platform, the PSF particles are sheet-like, for short reaction times, and fibrous for long reaction times, in contrast to spherical like particles for the polymer prepared using the conventional batch synthesis. The operating parameters of the VFD (rotational speed of the glass tube, its tilt angle and temperature) were systematically varied for establishing their effect on the molecular weight (M_w), glass transition temperature (T_g) and decomposition temperature, featuring gel permeation chromatography (GPC), differential scanning calorimetry (DSC) and thermal gravimetric analysis (TGA) respectively. The optimal VFD prepared PSF was obtained at 6000 rpm rotational speed, 45° tilt angle and 160 °C, for 1 h of processing with M_w ~10 000 g mol^{-1}, T_g ~158 °C and decomposition temperature ~530 °C, which is comparable to the conventionally prepared PSF.
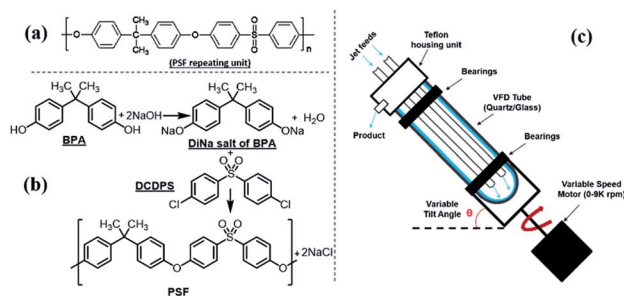
Introduction

Polymerisation reactions can be classified as arising from step-growth and chain-growth mechanisms, corresponding to condensation and addition reactions respectively.[1,2] Condensation polymers involve the reaction between two monomers in building the macromolecule, with or without the elimination of a small molecule such as water.[3,4] Among different types of condensation reactions, nucleophilic substitution features the most for preparing commercial organic polymers, such as in epoxide polymerisation,[3] or in the production of polysulfide rubbers from aliphatic dichlorides and sodium sulphide.[3,5]

Polysulfone (PSF) is a common thermoplastic polymer and a popular polymer incorporated in nano-filtration (NF) membranes. Aliphatic PSFs have unattractive physical properties including melting point and glass transition temperature, in contrast to PSFs incorporating aromatic moieties, which are prepared commercially via nucleophilic substitution reactions, Scheme 1a,[1,5] with the structure of a PSF repeating unit shown in the ESI.‡ Aromatic based PSFs feature in different applications, having desirable thermal,[6] chemical and mechanical

stabilities.[7,8] These polymers are also known as poly-ethersulfone (PESs) or polyphenylsulfone (PPSFs), depending on the nature of the backbone, Table 1.[1,9] The main difference between different types of PSF comes from the bisphenol (BP) repeating unit which controls certain properties, including glass transition temperature (T_g), Table 2.[1] Aromatic PSF is commercially obtained by condensation of equimolar quantities of 4,4′-dihalodiphenylsulfone (DHDPS) and a BP in the presence of a base.[1,5] This involves two separate steps, Scheme 1b; firstly, BPA is converted to the disodium salt (DiNa salt) by the addition of base, followed by a substitution reaction with dichlorodiphenyl-sulfone (DCDPS). Removal of water by-product generated in the first step is required to prevent hydrolysis of the DCDPS and facilitates the formation of higher molecular weight polymer.[1,5] Dimethyl sulfoxide (DMSO) and

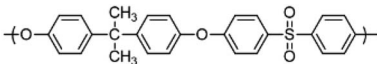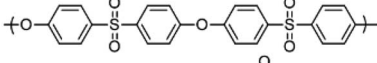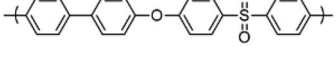[a]School of Engineering, Edith Cowan University, Joondalup, Perth, WA 6027, Australia
[b]Flinders Institute for Nanoscale Science and Technology, College of Science and Engineering, Flinders University, Adelaide, SA 5042, Australia. E-mail: colin.raston@flinders.edu.au

† Dedicated to Dr Ataollah Nosrati for his inspiration and leadership, who sadly passed away before publication.

‡ Electronic supplementary information (ESI) available: Experimental details and characterisation results (Fig. S1–S28). See DOI: 10.1039/d0ra00602e

Scheme 1 (a) Aromatic PSF repeating unit in PSF, (b) schematic of PSF synthesis involving nucleophilic substitution, and (c) diagram of the vortex fluidic device (VFD).[23]

Table 1 Chemical structure and glass-transition temperature, T_g, of PSF, PES, PPSF[1]

Polymer	Repeating unit structure	T_g, °C
Polysulfone (PSF)		185
Polyethersulfone (PES)		220
Polyphenylsulfone (PPSF)		220

sulfolane have been used to overcome the otherwise limited solubility of the DiNa salt of BPA under anhydrous conditions. Co-solvents such as chlorobenzene or toluene have also been used to increase the solubility of the salt.[1,5] Reaction temperatures $> \sim 120$ °C are effective in removing water from the reaction with >150 °C effective in driving the polymerisation to completion, and below this, low molecular weight sodium-capped oligomers precipitate on the internal surface of the reaction vessels.[5] Preparing PSF using conventional batch processing,[1,5] has some limitations, including that the processing is time consuming and energy intensive, and downstream processing is required to remove by-products.

We hypothesised that the high shear stress and intense micro-mixing in thin film microfluidics has potential to overcome these issues, imparting fast kinetics and with simplicity of the processing.[10,11]

The VFD, is a relatively new thin film microfluidic platform with a diverse range of applications, including graphene exfoliating, enhancing chemical reactivity and selectivity,[12,13] as in the synthesis of small molecule pharmaceuticals,[14,15] fabricating composite nanomaterials,[16] and controlling the pore size of mesoporous silica,[17] to mention a few. The rate of water evaporation in the VFD is dramatically increased, due to the large surface area of the thin film created inside the rapidly rotating VFD tube, and there is high heat and mass transfer, with improved reaction homogeneity, and when operating under continuous flow conditions, clogging is not an issue, unlike conventional channel based microfluidics.[18] It has also been used in preparing polymeric nanoparticles, notably polyethylenimine (PEI) nanoparticles[19] and cross linked bovine serum albumin (BSA) with glutaraldehyde,[20] and polymer coated superparamagnetic magnetite nanoparticles,[21] as well as manipulating the florescent properties of hyper-branched polymers.[22] The benefits of shear stress in the dynamic thin film in the VFD has not been explored for preparing PSF. This is addressed herein, while avoiding the use of potentially toxic reagents such as chlorinated co-solvents. This led to a new synthesis of the PSF, with the optimal conditions established by systematically exploring the operating parameter space of the VFD, including rotational speed, processing time, tilt angle of the tube, and temperature. The processing outcomes were also assessed relative to the glass transition temperature (T_g), molecular weight (M_w), particle size and shape, production yield and thermal stability of the PSF, in comparison with the polymer prepared using conventional batch processing. Different processing parameters in the VFD are likely to produce materials of different morphologies, which is important in the applications of PSF, such as in membrane fabrication.
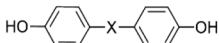
Experimental

Materials

All chemicals were used as received unless otherwise stated. High purity bisphenol A, [2,2-bis(4-hydroxyphenyl) propane], (BPA) (99%) and 4,4′-dichlorodiphenyl sulfone (DCDPS) (98%) and sodium hydroxide pellets (>97%) were purchased from Sigma Aldrich. Dimethyl sulfoxide (DMSO) (99.9%) and chlorobenzene (99.9%) were purchased from RCI Labscan Limited, with tetrahydrofuran (THF) (99.95%) purchased from ChemSupply. Ultrapure Milli-Q water was used for preparing aqueous solutions. DMSO was triple distilled before use and kept under nitrogen to limit adsorption of water. The vortex fluidic device (VFD) had a mounted heating block, effective in heating liquids in the tube, up to 175 °C.

PSF polymerisation

PSF was initially prepared according to the batch procedure[5] detailed in the ESI.‡ For VFD processing, BPA (228 mg, 1.0 mmol) and DMSO (1.0 mL) were placed in the VFD tube (20 mm

Table 2 T_g of PSFs formed from poly-condensation of DCDPS with various BP types

Bisphenol type	Structure	X	T_g, °C
4,4′-Dihydroxydiphenyl oxide		O	170
4,4′-Dihydroxydiphenyl sulfide		S	175
4,4′-Dihydroxydiphenyl methane		CH$_2$	180
2,2′-Bis(hydroxyphenyl)-propane		C(CH$_3$)$_2$	185

O.D., 17.5 I.D., 18.5 cm long) and rotated at 4000 rpm at 60 °C for 5 min, affording a clear colourless solution.

This reaction was also effective at room temperature, but the processing took 20 minutes. In contrast to the conventional method, no co-solvent was required. An aqueous solution of NaOH (103 μL, 50.2% w/w, 2 mmol) was then added to the tube, which was rotated at 4000 rpm, 45° tilt angle and 60 °C for 15 min. A solution of DCDPS (287 mg, 1 mmol) in DMSO (1.0 mL) was then added to the tube rotating at specific speeds (rpm), tilt angle (°), temperatures (°C), for specified times (min), for every designated experiment in Table S1 & Fig. S1.‡ At the end of each reaction, the sample was purified by filtration and any solid (NaCl by-product) discarded, whereupon, ethanol (10 mL) was added. The resulting coagulated white solid was washed twice and centrifuged (4 min, 805 RFC). The product was then filtered and dried for 2 h at 70 °C, affording PSF as a white solid, with the yield of product determined. In addition, for specific operational conditions, M_w, T_g and temperature variation profiles were determined at the optimal conditions, using gel permeation chromatography (GPC), differential scanning calorimetry (DSC) and thermal gravimetric analysis (TGA) respectively.

Characterization

The intermediate DiNa salt of BPA and the final VFD mediated PSF were characterized using NMR spectroscopy, recorded in DMSO-d_6 and CDCl$_3$ respectively (600 MHz Bruker instrument), and FT-IR spectroscopy (PerkinElmer ATR Fourier Transform spectrometer). ^{1}H-NMR spectra were acquired using a relaxation delay-time of 4 seconds. All chemical shifts are presented in ppm, using residual solvent as the internal standard. Scanning electron microscope (SEM) images were recorded on an Inspect FEI F50 SEM. Average molecular weights (M_w) and molecular weight distributions[24] were determined using a double detection Shimadzu GPC instrument equipped with an Ultraviolet (UV) and Refractive Index (RI) detectors. T_g and thermal stability measurements used a PerkinElmer DSC 8000 and TGA 8000 instrument, respectively, with instrument settings included in the ESI.‡ These properties were established for all polymers prepared in this study, in establishing the optimal operating parameters of the VFD, namely rotational speed (ω), tilt angle (θ), reaction time (t) and temperature (T). The optimal operational conditions are defined as those for forming the polymer with the highest T_g, M_w, thermal stability, and formed in the highest yield.

Results and discussion

The synthesis of PSF was conducted in the VFD and using batch processing for direct comparison on the effect of the unique fluid flow in the microfluidic platform. The production of the intermediate and final products was firstly confirmed using NMR and FTIR spectroscopy. Then the operating parameters of the VFD were systematically explored in mapping out how these affect the nature of the PSF with respect to T_g, M_w and thermal stability (DSC, GPC and TGA). Products were also studied for their morphological properties using SEM images.

Synthesis of DiNa salt of BPA

FT-IR and NMR spectroscopy[25] confirmed the formation of the DiNa salt of BPA and PSF, for both VFD and batch processing. The choice of solvent is critical for any process.[26] The DiNa salt of BPA, as the product of first step, is highly soluble in high boiling point DMSO (189 °C)[26] but this is difficult to remove for the isolation of the polymer and isolating the product to be characterized. In contrast, the DiNa salt is only sparingly soluble in THF, and to be able to isolate it for characterization purposes, this was the solvent of choice, with the precipitated salt washed with EtOAc. FTIR spectra of DiNa salt of BPA (Fig. S2a‡) obtained in the first step in the VFD, at ω 4000 rpm, θ 45° and T 60 °C for 5 min, clearly showed the removal of –OH stretching in forming the corresponding conjugate base, with peaks assignable to aromatic C=C (1508–1611 cm^{-1}), C–O (1050–1300 cm^{-1}) and C–H (1365–1465 cm^{-1}).[27,28] Peaks at 3000 cm^{-1} and above 3500 cm^{-1}, are attributed to THF[29,30] which can bind to metal centres, including sodium. ^{1}H-NMR of BPA in DMSO-d_6 (Fig. 1a) has peaks at ~1.53 and 9.13 ppm, assigned to the aliphatic protons and hydroxyl groups, respectively, with the later removed on reacting with base in forming DiNa. There are also peaks at 6.97 and 6.64 ppm corresponding to the aromatic protons of BPA (Fig. 1b).[31] Overall, changes in the ^{1}H-NMR spectra[30] are consistent with the formation of the DiNa salt (Fig. 1a) and the removal of water from the reaction mixture in the VFD. Such removal of water has been reported for the continuous flow synthesis of di-carboxylate esters synthesis.[18] For batch synthesis of DiNa, FTIR established that the longer the reaction time, the broader the –OH stretching peak, whereas for VFD processing the –OH stretching is smaller,[27,28] which is attributed to water dissipation in the VFD (Fig. S2b‡).

Synthesis of PSF

Fig. S3 and S4–S11‡ show the FTIR and NMR spectra for PSF prepared using both conventional[32] and VFD processing, as well as starting material for comparison. Fig. S10 and S11‡ show the
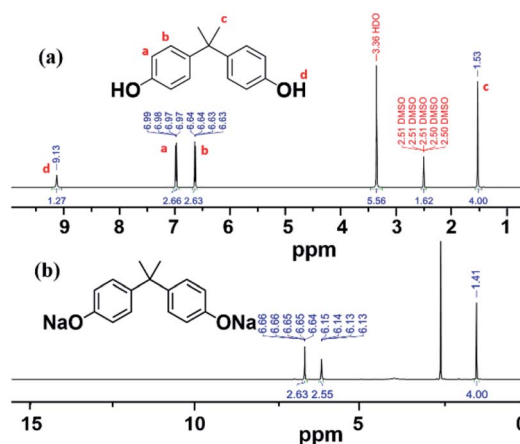

Fig. 1 ^{1}H-NMR spectra of (a) BPA and (b) DiNa salt of BPA obtained in the VFD in THF. ^{1}H-NMR measurements were recorded in DMSO-d_6.

^{1}H and ^{13}C NMR of VFD synthesized PSF at the optimised VFD condition, respectively, matching the corresponding spectra for highly porous PSF membranes.[33] The smaller peaks for the aromatic region in Fig. S10,‡ can be assigned to terminal groups of the polymer. In targeting the formation of high molecular weight polymer in the VFD, this region should be minimal.[33]

Varying VFD operational parameters

Experiments T_1 to T_6 in Table S1‡ were carried out to establish the effect of varying ω, from 3000 to 8000 rpm. Average molecular weight (M_w), T_g, and decomposition temperature, as well as yield were determined for all experiments. M_w, measured using GPC, were in the range ~2000 to ~11 000 g mol^{-1}, with the highest, ~4300 g mol^{-1}, formed at ω 6000 rpm, heating at 150 °C over 30 min, and θ 45° (T_4), with little change at higher speeds (Fig. 2a). DSC measurements to determine T_g were carried out under a nitrogen/air atmosphere, with the highest T_g reported thus far for PSF at ~187 °C.[33] T_g values for T_1, to T_6 were ~126, 125, 135, 142, 141, and 138 °C respectively, with the highest for PSF formed at 6000 rpm. The highest yield of isolated PSF, 53%, also corresponds to experiment T_4, with yields lower for increasing and reducing ω, at 37% and 39% for 3000 and 8000 rpm, respectively. The results clearly show that the properties of PSF (M_w and T_g) change on changing the rotational speed of the tube in the VFD, with 6000 rpm optimal, Fig. 2a.

Experiments T_7 to T_{12}, Table S1,‡ were at ω 6000 rpm, θ 45°, for 30 min at different temperatures. The effect of the choice of temperature impacts on the molecular weight of the PSF. There is clearly an effect on the temperature of the processing on the M_w of the polymer, and consequently T_g. The highest M_w and T_g

were for the PSF prepared at 170 °C, 12 000 g mol^{-1} and 168 °C, respectively, Fig. 2b. However, the yield of the isolated product dropped from 61% at 160 °C to 19.4% at 170 °C, and thus 160 °C reaction temperature was regarded as optimal, which is in accordance with temperature in conventional batch polymerisation (155 °C).[5] For experiments T_7 and T_8, at 80 and 120 °C respectively, there was no evidence for the formation of PSF.

Formation of PSF is incomplete at low temperature (T_7 & T_8), increasing up to 170 °C, resulting in a higher M_w and T_g. Temperatures higher than ~160 °C can result in solvent decomposition, discoloration or gelation of the reaction[5] and in this context we note that the yield of the product in the VFD drops at 170 °C. The T_g of batch prepared PSF in this research with M_w ~6300 g mol^{-1} was ~106 °C, significantly smaller than the PSF prepared in the VFD with the same M_w, summarised for entry T_{11}, Table S1,‡ M_w ~6300 g mol^{-1}, T_g ~152 °C. The relatively high T_g for such a low molecular weight PSF is noteworthy and highlights the novel process in the VFD under high shear.

The tilt angle, θ, in the VFD was varied from 0° (horizontal position) to 90° (vertical position) at intervals of 15°, entries T_{13}–T_{19}, Table S1.‡ There is a significant increase in yield from 21.7% at θ 30° to 59.2% at 45°, Fig. 2c. For θ at 30° and 90° the yields were also relatively high, at 58.3% and 58.1% respectively, but given the higher M_w (~7100 g mol^{-1}) and T_g (~153 °C) at θ 45°, this angle was regarded as optimal for the synthesis of PSF in the VFD, and this is in agreement with the outcome of optimisation studies for a number of applications of the device.[10–16,23] Understanding the complex fluid flow in general in the VFD is a challenge, and is a major focus of our current research.
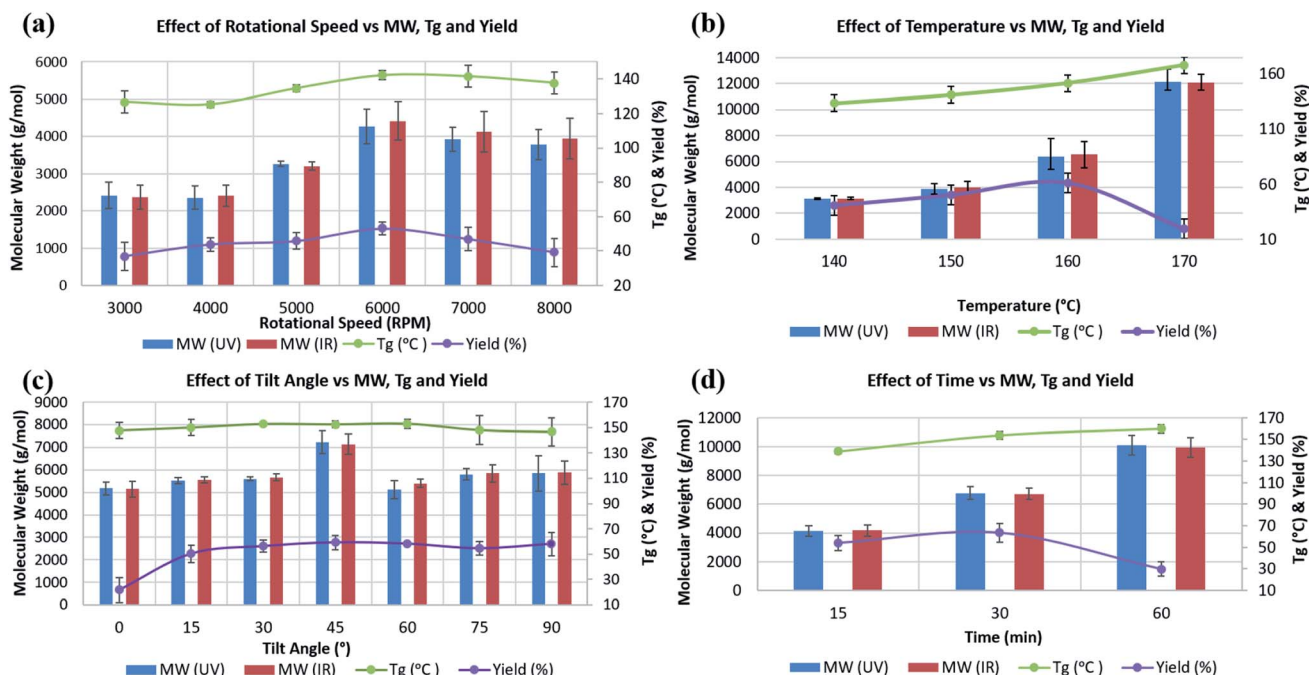

Fig. 2 Effect of VFD operating parameters on (a) rotational speed (rpm), (b) temperature (°C), (c) tilt angle (°), and (d) time (min) (horizontal axis) on the resulting M_w obtained from UV and IR detectors (blue and red histograms, respectively, in the left vertical axis), and on T_g and yield (%) (green and violet lines, respectively, in the right vertical axis).

The synthesis of PSF in the VFD was then carried out at 160 °C, with ω 6000 rpm and θ 45° for different processing times, entries T_{20}–T_{22}, Table S1.‡ M_w and T_g increased to ~10 000 g mol^{-1} and ~160 °C, respectively, by increasing the processing time up to 60 min. However, this resulted in a reduction in the yield, down to ~30% yield, in contrast to 63.7% for 30 min processing time, which has a lower M_w at ~6700 M_w, Fig. 2d. The lower molecular weight for shorter processing time is consistent with competing reactions, formation of the polymer *versus* its degradation under prolonged high shear. In this context, we note that polyethylenimine is broken down in the VFD.[19] GPC curves for commercial, conventional and VFD synthesized PSF at 6000 rpm, 160 °C, 45 tilt, and 60 min, now regarded as optimal conditions for processing in the VFD, are shown in Fig. 3a. The shorter retention time for commercial PSF is in agreement with its much higher M_w, ~60 000 g mol^{-1}, with M_w for conventional batch prepared PSF, M_w ~6000 g mol^{-1}, and that for PSF prepared in the VFD at optimal processing parameters, T_{22}, ~10 000 g mol^{-1}. The GPC results show a decrease in retention time of the VFD prepared PSF, the material having a higher M_w compared to the conventional batch prepared PSF. The

polydispersity index (PDI) for all these samples were 1.76, 1.78 and 1.76, respectively, and while they are similar, that prepared in the VFD has a narrower M_w distribution, and for the optimal processing parameters in general. In addition, PDIs for specific VFD optimised processing parameters are consistently lower, for example, in the optimal rotational speed, ω 6000 rpm, the PDI is 1.52, T_4, Fig. S12 and S13.‡ Lower PDIs for material generated in the VFD are associated with more uniform particle size distributions and highlight the benefit of using the VFD microfluidic platform, ESI (Fig. S14–S25‡). DSC thermograms in Fig. 3b are for commercial and conventional PSF, and optimised VFD fabricated PSF (ω 6000 rpm, 160 °C, θ 45°, and 60 min). All T_g values were collected from the second heating scan to minimise the effect of any evaporation of low volatiles or moisture. The heating curve of the VFD characterized PSF (black curve) has a glass transition at 157.9 °C (mid-point) with a change in the specific heat capacity, cp 0.213 J (g^{-1} °C). Conventional batch characterized PSF (red curve) has a lower T_g at 105.13 °C with cp 0.159 J (g^{-1} °C).

For all samples, the glass transition is superimposed by a small endotherm at 190.1, 108.5, and 160.4 °C, during heating scan, for commercial, conventional and VFD polymers, respectively. The DCS results (Fig. 3b) show a significantly higher T_g for the VFD prepared PSF compared to the conventional batch prepared PSF. This difference presumably relates to the intense micro-mixing and high shear rates in the VFD, and also the high rate of loss of water from the reaction mixture in the device, as established elsewhere.[18] However, the T_g for PSF prepared in the VFD is lower than that of commercial PSF (blue curve). Comparative DSC thermograms plots were also recorded in ascertaining the effect of ω on T_g, Fig. S26,‡ showing the best T_g measured is in accordance with the highest M_w polymer obtained at ω 6000 rpm (~142 °C) while it is ~125 and 137 °C at ω 4000 and 8000 rpm, respectively.

TGA measurements, carried out based on the setting suggested in Table S2, and Fig. S27,‡ establish a mass loss between 100 and 200 °C (DTG peak) of 7.4 and 0.5% for conventional VFD generated samples respectively, which is attributed to the loss of moisture and lower volatiles. The main decompositions of PSF for VFD processes T_9 (140 °C), T_{10} (150 °C), T_{11} (160 °C) and T_{12} (170 °C), conventional processes and commercial material, are at 530.0, 531.9, 533.0, 534.4, 534.6, and 536.4 °C (DTG Peak$_1$), with a mass loss of 68.7, 68.9, 68.9, 66.2, 65.0, and 66.2%, respectively (Fig. S27‡).

The results show that increasing the temperature up to 10 °C during the polymerization reaction has little effect on the main decomposition temperature, and accordingly M_w, T_g, and percent yield were more informative for optimising the processing in the VFD.

The morphology of PSF is important in its applications, for example, in membranes.[34,35] Fig. 4 shows SEM images for drop cast samples of commercial, conventional, and optimised VFD prepared PSF, and coated with ~5 nm layer of platinum. Commercial PSF has large globular shaped particles, *ca.* 30 μm in diameter, whereas that formed under batch processing herein are much smaller at submicron dimensions, Fig. 4(a and b), respectively. Interestingly, the size of the particles formed
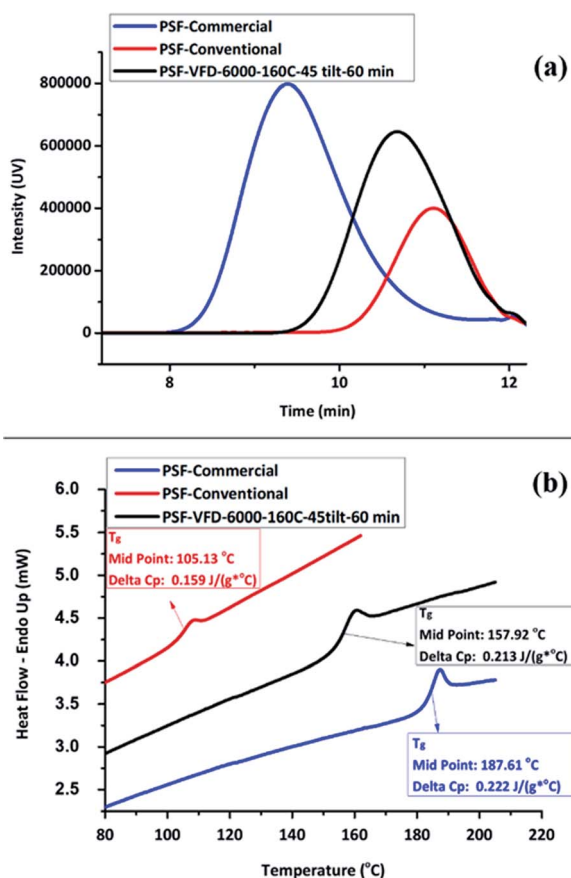

Fig. 3 Comparison between (a) GPC traces (UV detector) and (b) DSC thermograms of commercial, conventional and VFD synthesized PSF (T_{22} at 6000 rpm, 160 °C, 45°, and 60 min). (b) Temperature scan in T_g measurements were conducted between 30 °C and 230 °C at 10 °C min^{-1}.
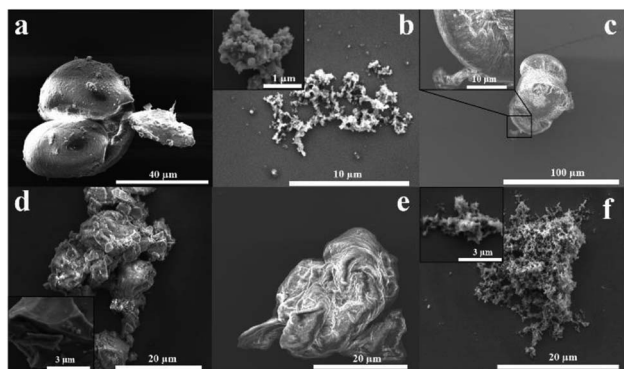
Fig. 4 SEM images of PSF for (a) commercial material, (b) material formed using conventional batch processing, (c) material formed in the VFD at the optimised conditions (T_{22} at 6000 rpm, 160 °C, 45°, and 60 min). PSF characterized in the VFD at 6000 rpm, 160 °C, θ 45° for (d) 15 min, (e) 30 min, and (f) 90 min reaction time. All the sample were drop cast and coated with *ca.* 5 nm layer of Pt.

under the optimised VFD processing conditions in the VFD, Fig. 4c, are similar to those of the commercial sample, yet the M_w of the material is significantly less, and the surface morphology is distinctly different. Also, of note is that PSF prepared away from optimised conditions in the VFD, Fig. 4(d–f) have different morphology and apparent particle size. For the shortest reaction time, 15 min, the product is sheet-like, Fig. 4d, changing to semi-spherical particles for 30 min, Fig. 4e, and fibrous material after 90 min, Fig. 4f. More images of the samples are shown in Fig. S28‡ in establishing that the images in Fig. 4 are representative of the bulk materials. The SEM images show that the mechanoenergy delivered into the dynamic thin film in the VFD perturbs the topology of the material, in being able to generate spherical, fibrous or sheet-like products, which is optimal at 6000 rpm, 160 °C, θ 45°, and understanding their formation is major challenge. The origin of this difference possibly relates to the complex fluid dynamics in the VFD becoming increasingly important over time, in moulding the polymer particles. This morphological variation is important in any downstream applications.

Conclusions

The preparation of PSF under high shear in the VFD using the confined mode of operation of the device has been established as an optimised process relative to M_w, T_g and percent yield, an and compared with commercially available material, and that prepared using conventional batch processing. The optimised VFD processing parameters were T 170 °C, ω 6000 rpm, θ 45° and t 30 min, which corresponds has M_w ~12 000 g mol^{-1}, T_g 168 °C and decomposition temperature ~530 °C. However, the lower yield (18%) at this temperature, 160 °C was deemed more optimal, affording M_w ~7000 g mol^{-1}, T_g ~154 °C, and ~64% yield, and for a longer reaction time, 60 min, now affording M_w ~10 000 g mol^{-1} and T_g ~ 158 °C. While the latter results in a lower yield (~30%), the reaction time can be defined based on the importance of either the M_w or yield of the process.

The VFD prepared PSF has comparable properties relative to that prepared using conventional batch processing, with M_w ~6000 g mol^{-1}, but this is smaller than that of commercially prepared PSF, ~60 000 g mol^{-1}. However, our approach in avoiding the use of toxic reagents such as chlorinated co-solvents (chlorobenzene) is an advance in the field, in endeavouring to develop sustainable technologies. The ability to remove water *in situ* is also an important part of using the VFD relative to batch processing, in avoiding termination reactions. Also important is the processing time, in changing the morphology of the particles, which may be important in downstream applications. Indeed, the lower M_w VFD material may open new particle size/chain length specific applications of PSF, further tuned by morphology considerations, sheet like *versus* globular like particles. We note that the fluid dynamics in the VFD is inherently complex and that this determines the rate of the reactions (high shear and intense micro-mixing) as well as the shape, determined by how the fluid actually flows in the device. This is a major research effort underway involving a number of laboratories. The reduction in percent yield for increasing processing time may arise also from the shear stress resulting in bond cleavage and reduction in the length of the polymer chain. In this context, it is noteworthy that the VFD is effective in breaking down polyethylenamines.[19]

Conflicts of interest

There are no conflicts to declare.

Acknowledgements

Notes and references

1 K. Othmer, *Encyclopedia of Chemical Technology*, Wiley, New York, 4th edn, 1996, p. 19.

2 D. A. Schlüter, C. Hawker and J. Sakamoto, *Synthesis of polymers, new structures and methods*, Wiley-VCH Verlag GmbH & Co. KGaA., Weinheim, Germany, 2012.

3 F. W. Billmeyer, *Textbook of polymer science*, John Wily & Sons Inc., New York, 3rd edn, 1984.

4 M. K. Saraf, MSc Thesis, North Carolina State University, 2001.

5 R. N. Johnson, A. G. Farnham, R. A. Clendining, W. F. Hale and C. N. Merriam, *J. Polym. Sci., Part A-1: Polym. Chem.*, 1967, **5**, 2375–2398.

6 S. Zhu, G. Xiao and D. Yan, *J. Polym. Sci., Part A: Polym. Chem.*, 2001, **39**, 2943–2950.

7 M. J. Jung, J. Parrondo, C. G. Arges and V. Ramani, *J. Mater. Chem. A*, 2013, **1**, 10458–10464.

8 M. Ciobanu, L. Marin, V. Cozan and M. Bruma, *Rev. Adv. Mater. Sci.*, 2009, **22**, 89–96.

9 B. Van der Bruggen, *J. Appl. Polym. Sci.*, 2009, **114**, 630–642.

10 X. Chen, J. F. Dobson and C. L. Raston, *Chem. Commun.*, 2012, **48**, 3703–3705.

11 L. Yasmin, X. Chen, K. A. Stubbs and C. L. Raston, *Sci. Rep.*, 2013, **3**, 2282.

12 J. Britton, J. M. Chalker and C. L. Raston, *Chem.–Eur. J.*, 2015, **21**, 10660–10665.

13 L. Yasmin, K. A. Stubbs and C. L. Raston, *Tetrahedron Lett.*, 2014, **55**, 2246–2248.

14 M. N. Gandy, C. L. Raston and K. A. Stubbs, *Org. Biomol. Chem.*, 2014, **12**, 4594–4597.

15 C. L. Tong, U. H. Stroeher, M. H. Brown and C. L. Raston, *RSC Adv.*, 2015, **5**, 7953–7958.

16 F. M. Yasin, R. A. Boulos, B. Y. Hong, A. Cornejo, K. S. Iyer, L. Gao, H. T. Chua and C. L. Raston, *Chem. Commun.*, 2012, **48**, 10102–10104.

17 C. L. Tong, R. A. Boulos, C. Yu, K. S. Iyer and C. L. Raston, *RSC Adv.*, 2013, **3**, 18767–18770.

18 J. Britton, S. B. Dalziel and C. L. Raston, *Green Chem.*, 2016, **18**, 2193–2200.

19 X. Luo, A. H. M. Al-Antaki, S. Pye, R. Meech, W. Zhang and C. L. Raston, *ChemPhotoChem*, 2018, **2**, 343–348.

20 X. Luo, A. H. M. Al-Antaki, D. P. Harvey, Y. Ruan, S. He, W. Zhang and C. L. Raston, *ACS Appl. Mater. Interfaces*, 2018, **10**, 27224–27232.

21 N. J. D'Alonzo, P. K. Eggers and C. L. Raston, *New J. Chem.*, 2017, **41**, 552–558.

22 J. Tavakoli, N. Joseph, C. L. Raston and Y. Tang, *Nanoscale Adv*, 2020, **2**, 633–641.

23 S. J. Pye, S. J. Dalgarno, J. M. Chalker and C. L. Raston, *Green Chem.*, 2018, **20**, 118–124.

24 *Handbook of Polymer Synthesise, Characterization, and Processing*, ed. E. Saldivar-Guerra and E. Vivaldo-Lima, Wiley, New Jersey, 2013.

25 O. Agboola, J. Maree and R. Mbaya, *Environ. Chem. Lett.*, 2014, **12**, 241–255.

26 S. P. Zala, K. P. Patel, K. S. Patel, J. P. Parmar and D. J. Sen, *Int. J. Drug Dev. Res.*, 2012, **04**, 41–55.

27 M. M. Alavi Nikje and M. Askarzadeh, *Polímeros*, 2013, **23**, 29–31.

28 T. Zou, S. Li, W. Huang and X. Liu, *Des. Monomers Polym.*, 2012, **16**, 25–30.

29 A. Dwivedi, V. Baboo and A. Bajpai, *J. Theor. Chem.*, 2015, **2015**, 1–11.

30 G. R. Fulmer, A. J. M. Miller, N. H. Sherden, H. E. Gottlieb, A. Nudelman, B. M. Stoltz, J. E. Bercaw and K. I. Goldberg, *Organometallics*, 2010, **29**, 2176–2179.

31 P. N. Shah, N. Kim, Z. Huang, M. Jayamanna, A. Kokil, A. Pine, J. Kaltsas, E. Jahngen, D. K. Ryan, S. Yoon, R. F. Kovar and Y. Lee, *RSC Adv.*, 2015, **5**, 38673–38679.

32 G. Nechifor, Ș. I. Voicu, A. Nechifor and G. Sorina, *Desalination*, 2009, **241**, 342–348.

33 Y. Xie, N. Moreno, V. M. Calo, H. Cheng, P.-Y. Hong, R. Sougrat, A. R. Behzad, R. Tayouo and S. P. Nunes, *Polym. Chem.*, 2016, **7**, 3076–3089.

34 M. Elimelech, X. Zhu, A. E. Childress and S. Hong, *J. Membr. Sci.*, 1997, **127**, 101–109.

35 X. Fu, T. Maruyama, T. Sotani and H. Matsuyama, *J. Membr. Sci.*, 2008, **320**, 483–491.